SUBSTRATE BARRIER EFFECTS FOR A R-19 FIBROUS INSULATION BATT

K.T. Harris[+], T.A. McCarty[*], J.A. Roux[#]
Department of Mechanical Engineering
University of Mississippi
University, MS 38677

ABSTRACT

This research investigates the effects on the total heat transfer when various substrate barriers are implemented at the bottom of a R-19 fiberglass insulation batt. A plastic (polyethylene) vapor barrier, perforated and non-perforated radiant barriers are investigated. Heat transport in ceiling insualtion is assumed to be transferred by these three mechanisms: conduction and radiation heat transfer and moisture transport (please note convection heat transfer is not considered in this investigation). By modeling each of these three modes of heat transfer at the attic insulation substrate, the total heat transfer into the house (summer conditions) can be obtained. Further modeling can determine the changes in the three individual modes of heat transfer once a substrate barrier is added. Summertime experimental data were collected at an occupied North Mississippi residence for cases with and without a vapor barrier at the substrate for R-19 fiberglass insulation. Predictions were made by a transient numerical/analytical model that simultaneously combines conduction and volumetric radiation heat transfer and moisture transport to obtain the total heat transfer at the substrate. Experimentally and predicted total heat transfer results are compared. Profiles such as temperature-time histories and vapor H_2O concentrations are presented to support the experimentally determined effects on the overall heat transfer at the substrate.

[+]Graduate Student; [*]Assistant Professor; [#]Professor

INTRODUCTION

It has been shown in previous works [1-4] for humid southeastern summertime conditions that moisture can cause a significant increase in the total heat transfer. A literature survey and private information [5-7] indicated that despite knowledge on moisture effects on heat transfer there is little knowledge on the impact of adding different substrates, i.e. when a plastic vapor barrier is added to the substrate. This study investigated the effect of a plastic vapor barrier or a foil radiant barrier has on the overall heat transfer through the R-19 fiberglass insulation batt. Experimental data with and without these barriers were collected and compared to the results of an analytical/numerical model. Furthermore the model was used to investigate the three modes of heat transfer (conduction, radiation heat transfer and moisture transport, no convection was considered) to determine whether or not each mode of heat transfer would be affected by changes in the others.

The effect of foil radiant barriers placed at the top of the batt has been discussed in previous work [3-4]. However, in this study a theoretical investigation of adding a non-perforated foil radiant barrier and a perforated foil radiant barrier to the substrate of the insulation batt was conducted. Numerous attempts were made to find information on the subject matter of employing a radiant substrate barrier but none has been found [5-7]. The analytical/numerical model was used to illustrate how the different modes of heat transfer are affected and/or altered by the addition of a foil radiant substrate barrier. Will the total heat transfer increase or decrease with the addition of a substrate barrier is a question that will be answered in this study; as well as how the individual heat transfer modes would be impacted. Both a perforated and a non-perforated radiant barrier were modeled as a batt substrate barrier

in this study. Experimental temperature and relative humidity data obtained for the plastic vapor barrier case were used for the input parameters in the numerical/analytical model for the non-perforated foil radiant barrier substrate simulation and data obtained from the no plastic vapor barrier case were used as the input parameters for simulating the perforated radiant barrier substrate case.

EXPERIMENTAL SETUP

Shown in Fig. 1 is the attic geometry for the experimental setup corresponding to the North Mississippi residence where data were collected. The insulation top boundary is the attic air and the substrate boundary is gypsum board for the cases without a vapor or radiant barrier at the bottom of the insulation. Experimental data were recorded for the case of a plastic (polyethylene - 6 mil) vapor barrier, but only predictions were made for the case of a radiant substrate barrier. The subscripts s, o, a, and r represent the substrate (bottom of the insulation batt), the insulation top, the attic air, and the roof respectively. Also it should be noted that the coordinate system originates at the substrate where $y=0$ and hence at the top of the insulation batt $y=y_o$.

Data were collected for a horizontally oriented R-19 fiberglass insulation batt. All experimental data were recorded every 15 minutes using an HP 3528A data acquisition system. All data channels were sampled 100 times at each 15 minute data acquisition interval in order to improve the signal/noise ratio. Temperatures (see Fig. 2) were measured with type-J thermocouples that are stated to be accurate to $\pm 1/4$ K. Relative humidities were measured with Hycal CT-829-A-RX temperature compensated relative humidity (R.H.) meters (see Fig. 2) that are accurate to less than 1% between $20 < \text{R.H.} < 80\%$. Heat fluxes were measured with the

Hycal BI-7-20-WP-J-X-X6 high sensitivity heat flux meters (see Fig. 2); the heat flux meters were calibrated by Holometrix Inc. and are stated to be accurate to $\pm 5\%$ of full scale (heat flux of 7.8 W/m^2). The heat flux meters were located at the interface between the fiberglass batt and gypsum board at the substrate; when a vapor barrier was employed at the substrate, a heat flux meter was placed between the fiberglass and vapor barrier and another heat flux meter was placed between the vapor barrier and the gypsum board. For all cases these two heat flux meters showed excellent agreement (less than 3% difference).

NUMERICAL/ANALYTICAL MODEL

The basic equations for the numerical/analytical model are the radiative transport equation, the species equation, and the energy equation. To simplify the model, the attic insulation is considered to behave like a plane parallel layer and the primary assumptions are given as follows: 1) transient, one-dimensional combined conduction, radiation heat transfer with mass (H_2O) diffusion, and adsorption/desorption of H_2O; 2) volumetric radiation within the fiberglass insulation which was considered as an absorbing, emitting and scattering (isotropic) medium; 3) gray radiative properties (extinction coefficient and albedo); 4) convection is neglected; 5) relative humidities and temperatures at the boundaries are known (measured) functions of time.

This work also considers the heat of H_2O adsorption to be equal to the heat of H_2O desorption and it neglects the small hystersis phenomenon present between the adsorption and desorption isotherms. The density of the fiberglass insulation was taken to be 12 kg/m^3 [8]. The temperatures at the insulation top, bottom, and roof are the required boundary condition information for solving the energy equation and the radiative transport equation. The boundary

temperatures and relative humidities are required for obtaining concentrations of bound H_2O and vapor H_2O species which are needed for solving the species equations. Emissivities are specified at the roof ($\epsilon_n = 1-\rho_n = .85$) and substrate ($\epsilon_s = 1-\rho_s = .95$) for the no barrier and plastic vapor barrier surfaces and ($\epsilon_s = 1-\rho_s = .05$) for the radiant barrier case [9]. That thermal/radiative properties used in this model are presented in Table 1.

Radiative Transport Equation

The radiative heat flux, q_r, is required for solving the energy equation, Eq. (6); it is obtained by solving the radiative transport equation as presented below. The one-dimensional axially symmetric radiative transport equation for an absorbing, emitting, and anisotropically scattering medium from Ref. [10] can be written as

$$\mu \frac{dI(\tau,\mu)}{d\tau} = -I(\tau,\mu) + \frac{\omega}{2}\int_{-1}^{1} I(\tau,\mu')\ \Phi\ (\mu,\mu')\ d\mu' + n^2(1-\omega)\ I_b(T(\tau)) \quad (1)$$

Here, τ ($\tau = \beta y$ and β is the extinction coefficient) is the optical depth, μ is the cosine of the polar angle Θ, ω is the single scatter albedo, n is the refractive index of the medium, $I(\tau, \mu)$ is the radiative intensity at depth τ in the specified direction of μ, I_b is the emitted radiative intensity at depth τ, $\Phi(\mu, \mu')$ is the scattering function or phase function; here $\Phi(\mu, \mu') = 1$ for isotropic scattering.

The boundary conditions for the Eq. (1) are given by

$$I(0,\mu) = \rho_s I(0,-\mu) + (1-\rho_s)n^2 I_b(T_s), \qquad \mu > 0$$
$$I(\tau_o,-\mu) = \rho_n I(\tau_o,+\mu) + (1-\rho_n)n^2 I_b(T_R), \quad \mu > 0$$

where $I_b(T_R)=e_b(T_R)/\pi$ and for a gray body $e_b(T_R)=\sigma T_R^4$. Here, ρ_s is the reflectivity of the substrate and ρ_n is the reflectivity of the roof for the no foil above the insulation case. If a foil radiant barrier is used above the insulation, then ρ_n is the reflectance (.95) of the foil and T_R is the top of the batt temperature T_o. It should be noted that n=1 for this problem. A quasi-analytical technique with the method of discrete ordinates, employing a 16 point Gaussian quadrature, was used in solving the radiative transport equation (Eq. (1)) and the details can be found in Refs. [10,11]. The radiative heat flux needed in Eq. (6) is given by definition as

$$q_r(\tau) = \int_0^{2\Pi} \int_{-1}^{1} I(\tau,\mu)\mu d\mu d\psi \tag{2}$$

Species Equations

For one-dimensional unsteady moisture transport, the species conservation equation for bound H_2O (H_2O which exists within the fiberglass binder) can be expressed as

$$\frac{\partial m_b}{\partial t} - \frac{\partial}{\partial y}\left(\gamma_b \frac{\partial m_b}{\partial y}\right) = \dot{m}_b \tag{3}$$

Here, m_b (kg/m^3) is the concentration of bound H_2O, γ_b is the diffusion coefficient, $\dot{m}_b$ is the rate of adsorption/desorption of bound H_2O (sink/source term). Similarly, the species conservation equation for vapor H_2O can be written as

$$\frac{\partial m_v}{\partial t} - \frac{\partial}{\partial y}\left(\gamma_v \frac{\partial m_v}{\partial y}\right) = \dot{m}_v \tag{4}$$

In the above equation, all the terms denote the same meaning as in Eq. (3) except that the subscript "v" denotes vapor H_2O. The source terms ($\dot{m}_b$,$\dot{m}_v$) in Eqs. (3) and (4) account for

H_2O adsorption/desorption. The H_2O mass sorption isotherms are given in Ref. [12]. Since the heat of adsorption and desorption for the phenolic binder are not readily available, it is considered that the binder's heat of adsorption and desorption acts as zeolite whose properties for H_2O are known [13,14]. It should be noted that the rate of adsorption of bound H_2O is equal to rate of desorption of vapor H_2O and vice versa. Therefore, the source terms are given by

$$\dot{m}_b = - \dot{m}_v = \rho_f \frac{\partial X}{\partial t} \tag{5}$$

where

$$\frac{\partial X}{\partial t} = m_\phi \frac{\partial \phi}{\partial t} \tag{5a}$$

In Eq. (5a), m_ϕ is a constant obtained from the data presented in Ref. [12] and is given in Table 1. The symbol ϕ is the relative humidity and Eqs. (5) and (5a) yield the moisture mass adsorption/desorption as a function of the relative humidity in accordance with Ref. [15] which reported the adsorption isotherm to be a function of relative humidity only and not a separate function of temperature. The quantity X is dimensionless and has units of kg H_2O/kg dry fiberglass.

The boundary conditions for Eqs. (3) and (4) are given by

$$m_b = (m_b)_s(t); \quad m_v = (m_v)_s(t) \quad \text{at} \quad y = 0$$

$$m_b = (m_b)_o(t); \quad m_v = (m_v)_o(t) \quad \text{at} \quad y = y_o$$

where $(m_b)_s(t)$, $(m_v)_s(t)$ are the mass concentrations of bound H_2O and vapor H_2O at the

substrate; $(m_b)_o(t)$, $(m_v)_o(t)$ are the mass concentrations of bound H_2O and vapor H_2O at the top of the insulation batt; these concentrations were determined from the measured relative humidity and dry-bulb temperature at the bottom and top of the insulation batt. Linear vapor H_2O and bound H_2O concentration profiles were chosen as the initial concentration conditions (midnight, t=0).

Energy Equation

The one-dimensional energy equation for transient, coupled conduction, radiation heat transport, diffusion of vapor H_2O and bound H_2O, and adsorption/desorption of H_2O is given by

$$\frac{\partial}{\partial y}\left(k_f \frac{\partial T}{\partial y}\right) - \frac{\partial q_r}{\partial y} + \frac{\partial}{\partial y}\left(\gamma_v\, i_v \frac{\partial m_v}{\partial y}\right) + \frac{\partial}{\partial y}\left(\gamma_b\, i_b \frac{\partial m_b}{\partial y}\right) + \dot{q} = \rho_f c_f \frac{\partial T}{\partial t} \qquad (6)$$

where

$$\dot{q} = h_{ad}\dot{m}_b \qquad (6a)$$

with boundary conditions:

$$T = T_s(t) \text{ at } y = 0$$

$$T = T_o(t) \text{ at } y = y_o$$

Where $T_s(t)$ is the measured temperature at the bottom of the fiberglass batt as a function of time and $T_o(t)$ is the measured temperature at the top of the fiberglass batt as a function of time. A linear temperature profile was chosen as the initial temperature condition (midnight, t = 0). The terms on the left hand side of the Eq. (6) represent heat conduction, volumetric radiation, diffusion of vapor H_2O and bound H_2O, and the heat source/sink due to H_2O adsorption/

desorption within the insulation binder respectively, whereas the term on the right hand side represents the transient term. In Eq. (6), k_f is the thermal conductivity of the insulation, ρ_f is the bulk density of the insulation, c_f is the specific heat of the insulation. The symbols γ_b and γ_v are the diffusion coefficients and i_b and i_v are the specific enthalpies of the bound H_2O and vapor H_2O respectively, h_{ad} (Eq. (6a)) is the heat of H_2O adsorption/desorption and $\dot{m}_b$ was defined in Eq. (5). The total heat flux for the no plastic vapor barrier case or the perforated radiant substrate barrier case is given by the following

$$\hat{q}_T = -k_f \frac{\partial T}{\partial y}\Big)_{y=0} + q_r(0) - \gamma_v \frac{\partial m_v}{\partial y} i_v\Big)_{y=0} - \gamma_b \frac{\partial m_b}{\partial y} i_b\Big)_{y=0} \quad (7a)$$

where the first term i s the conduction term, the second the radiation term, the third the diffused H_2O vapor term, and the fourth the diffused bound H_2O term. It was assumed that the perforated radiant barrier substrate did not retard the diffusion of vapor H_2O through the barrier in any way. Equation (7b) below is used when a plastic or non-perforated radiant vapor barrier is implemented at the substrate

$$\hat{q}_T = -k_f \frac{\partial T}{\partial y}\Big)_{y=0} + q_r(0) - \gamma_v \frac{\partial m_v}{\partial y} h_{ad}\Big)_{y=0} \quad (7b)$$

It can be seen that Eqs. (7a) and (7b) are similar in that they both have the conduction and radiation terms but differ in that once a vapor (plastic or non-perforated radiant) barrier is in place the vapor cannot be transported through the substrate/fiberglass interface, hence the H_2O mass transfer term in Eq. (7b) represents the mass flow (absorbed/desorbed) into and out of the phenolic binder at the bottom of the batt.

Solution Scheme

Equations (1),(3),(4) and (6) were solved simultaneously by an iterative scheme that employs a control volume based finite difference method (Patankar method [16]). The transient solution is obtained by marching forward in time with an appropriate time step (5 min time step). A time step that yielded no change in the converged temperatures and species concentrations was considered an appropriate time step. A non-uniform spatial grid with 17 nodal points was used in the program to achieve lower computational time without sacrificing accuracy; the computation time on an IBM 3084 to predict all the results for a 24 hour period was about 30 seconds of CPU time. It should be noted that the experimental data were recorded every 15 minutes and hence a linear interpolation was used to input boundary condition information at the 5 minutes time step intervals which occur in between the 15 minute data acquisition intervals for the experimental data.

RESULTS

Vapor Barrier

The following results are those of a typical Northern Mississippi summer day. Figure 3 is the temperature-time history profiles for the 24-hour time period of July 27,1994. This figure shows the roof (T_R), top of the batt (T_o), attic air (T_A) (2" above the batt), and the bottom of the batt (T_S) temperatures in which the T_R, T_o, and T_S were used as boundary conditions for the numerical/analytical model. The figure shows that the top of the batt and attic air temperatures were both higher than the bottom of the batt temperature for the heating portion of the day ($\approx$550 min. - 1200 min.). This indicates that during the heating portion of the day the temperature gradient was such that heat would be transferred into the house.

Figure 4 shows the measured relative humidity at the top and bottom of the R-19 insulation batts for both with and without a plastic vapor barrier at the substrate. The relative humidities at the top of the batt for both cases are practically identical. The top of the batt relative humidities are higher during the early morning ($\approx$0 min. - 550 min.) and drop off rapidly during the heating portion of the day as expected. However, in comparing the bottom of the batt relative humidities for the two batts it can be seen that the batt with a plastic vapor barrier has a significantly higher relative humidity measurement than the one without a vapor barrier. The relative humidity levels in the attic region never become high enough to reach the dew point, therefore condensation risks are not relevant for Northern Mississippi where our data were collected for summer and winter conditions. The highest relative humidity level recorded in the attic has never been greater than 85%. Shown in Figure 5 are the dimensionless vapor H_2O concentration histories for batts both with and without a vapor barrier. Examining the insulation batt without a vapor barrier, the vapor concentration at the top of the batt is always greater than that at the substrate; hence for this batt there is always a gradient between the top and bottom of the batt such that there will be a diffusion of vapor H_2O from the top of the batt to the bottom. Figure 5 also reveals that for the batt with a plastic vapor barrier, the H_2O vapor concentration gradient between the top and bottom of the batt at any given time is quite small; hence diffusion of vapor H_2O within the insulation batt is significantly decreased with the implementation of the plastic vapor barrier. With the above temperature profiles (Fig. 3) and concentration profiles (Fig. 5) employed as boundary conditions, the total predicted and measured heat fluxes for batts both with and without a plastic vapor barrier are compared in Fig. 6. This figure shows that there is good agreement between the numerical/analytical model and

the experimental data. All four sets of results display a predominantly negative heat flux which would indicate that heat would be transferred towards the substrate and into the living space of the residential home. In comparing the batt with a plastic vapor barrier to that without a barrier, it is seen that the total heat transfer at the substrate has been reduced somewhat for the plastic vapor barrier case. Furthermore, Table 2 shows the integrated values for both batts and it is found that the substrate heat transfer is reduced by 13% (comparing the experimental data) during the heating portion of the day with the utilization of a plastic vapor barrier.

Figure 7 demonstrates the additional usefulness of the numerical/analytical model, that is, with this model the three modes of heat transfer can be individually analyzed. Figure 7 depicts how the three different modes of heat transfer (conduction, radiation, and H_2O vapor diffusion) are affected once a plastic vapor barrier is in place at the substrate. The moisture mode of heat transfer due to vapor H_2O diffusion was reduced over the entire 24-hour period with the use of a plastic vapor barrier. When a plastic vapor barrier is used, the H_2O vapor is not permitted to diffuse through the substrate and into the living space but is adsorbed or desorbed throughout the entire batt. It should be noted that some adsorption and desorption occurred near the substrate within the fiberglass insulation phenolic binder. In other words near the substrate, the phenolic binder acts as an desiccate and adsorbs or desorbs the vapor H_2O. Although a plastic vapor barrier is in place, Fig. 7 shows that a small vapor H_2O diffusion gradient exists at the substrate which is associated with adsorption and desorption into and out of the phenolic binder and not mass diffusion through the plastic barrier. The conduction and radiation modes are both reduced slightly once a plastic vapor barrier is incorporated. This is because once a vapor barrier is used the mass transfer is reduced and hence the energy

associated with the mass transfer is reduced, therefore changing the temperature field near the substrate which slightly decreases the conduction and radiation modes of heat transfer. Figure 8 displays spatial vapor H_2O concentration profiles at different times of the 24-hour period for both batts. The spatial concentration profiles for no vapor barrier at the 225 and 990 minute time instances are identical because the temperature and relative humidity gradients between the top and bottom of the batt are the same for these time instances. For each of these time instances the batt without a plastic vapor barrier has a higher concentration gradient at the substrate while the profile of the batt with a plastic vapor barrier is relatively constant. This would imply that with a plastic vapor barrier, the vapor H_2O diffusion remains small throughout the batt. Figure 7 showed that all three modes of heat transfer were reduced with the addition of a plastic vapor barrier and Fig. 8 displays that the vapor H_2O concentration profiles are almost uniform once a plastic vapor barrier has been added; combining the results of these two figures illustrates why the overall substrate heat transfer was reduced in Fig. 6 with the implementation of a plastic vapor barrier.

Radiant Barrier Substrate

The following results are predictions for batts with a perforated foil and non-perforated foil radiant barrier at the substrate. No experimental data were obtained for these two cases. The non-perforated foil radiant barrier was considered to act as a vapor barrier. While a batt without any vapor barrier at the substrate was used to simulate the case with a perforated foil radiant barrier. Plastic vapor barrier and non-vapor barrier temperature and relative humidity data from the previous section of this paper were used as input for the numerical/analytical model for the non-perforated and perforated foil radiant substrate barriers, respectively. The

substrate reflectivity (ρ_s) within the numerical/analytical model was changed from that of a gypsum board or plastic interface (ρ_s= .05) to that of an aluminum foil interface (ρ_s= .95). Figure 9 depicts the overall predicted substrate heat flux-time histories for the non-perforated radiant barrier batt compared to the predicted heat flux-time histories for the plastic vapor barrier batt from Fig. 6 and also shown is the measured plastic vapor barrier data from Fig. 6. All three sets of results show close agreement which implies that the non-perforated foil radiant barrier does yield basically the same results as a plastic vapor barrier. The total predicted heat flux at the substrate did not significantly change (less than 1%) when a non-perforated foil radiant barrier was added as compared to the plastic vapor barrier. Again the usefulness of the numerical/analytical model shows that even though the total heat transfer at the substrate did not change in Fig. 9, it can be seen in Fig. 10 that there was a change in the three modes of heat transfer. Investigating Fig. 10 one can see that the radiation mode of heat transfer is practically eliminated once a non-perforated foil radiant barrier is added to the substrate. The radiant energy that was associated with the radiation mode of heat transfer for the plastic vapor barrier case is now (non-perforated radiant barrier) reflected from the substrate back into the insulation batt where this energy is absorbed and causes an increase in the conduction mode of the total heat transfer. The conduction mode for the non-perforated radiant barrier case was increased by the same amount that the radiation mode was decreased when compared to the plastic vapor barrier case. The heat transfer due to H_2O transport was not significantly affected by this predicted implementation of a non-perforated foil radiant barrier. The net effect is that there is essentially no change in the total substrate heat transfer, but the radiation and conduction modes are strongly altered.

Figure 11 depicts a comparison between the predicted perforated radiant barrier batt and that of the measured and predicted no vapor barrier batt (Fig. 6). Over the entire 24-hour period there is no significant difference between the three sets of results. The total substrate heat transfer for the predicted cases of either a perforated foil radiant barrier or no vapor barrier are practically identical. There was almost no change in the total heat transfer; however, in Fig. 12 it can be seen that the radiation mode of heat transfer was reduced drastically for the perforated radiant barrier case when compared to the case without any substrate barrier. This nullification of the radiation mode causes an increase in the conduction mode because the radiant energy is reflected back into the insulation batt and is absorbed by the fiberglass and then is changed into conduction heat transfer. As shown in Fig. 12, the conduction mode of heat transfer increased considerably with the addition of a perforated foil radiant barrier at the substrate. The vapor H_2O diffusion mode of heat transfer did not change for the case with a perforated radiant barrier as compared to the case with no vapor barrier. Since the vapor H_2O diffusion mode did not change and the changes in the conduction and radiation modes offset one another, the total heat transfer at the substrate did not change with the use of a perforated radiant barrier when compared to a case with no vapor barrier.

Vapor Barrier at Substrate and Radiant Foil Barrier Above

Previous works [3-4] showed that the total substrate heat flux can be reduced as much as 42% once a radiant foil barrier is above a R-19 fiberglass insulation batt. This investigation showed that the total substrate heat flux can be reduced by 13% once a plastic vapor barrier is added to the substrate of a R-19 fiberglass insulation batt. It would appear that a combination of these two barriers (plastic below and foil above) would yield an increased reduction in

substrate heat flux. Figure 13 illustrates this by showing the results of the total substrate heat flux for June 25, 1994 when the combination of a plastic vapor barrier at the substrate and a foil radiant barrier above are employed; this combination is compared to a insulation batt without a vapor barrier at the substrate and no radiant barrier above (i.e. standard batt). The integrated heat fluxes over the heating portion of the day are tabulated in Table 2, the heat flux at the substrate is reduced by 53% when compared to the standard insulation batt.

It should be noted that only representative data have been shown for all of the cases above; however numerous days of data were obtained for all of the experimental conditions. The experimental data confirms the results presented in this paper over a time period of many weeks.

CONCLUSIONS

This paper has presented an investigation of the changes in the total heat transfer and the changes in the different modes of heat transfer (conduction, radiation and moisture transport) when a plastic vapor barrier, a non-perforated foil radiant barrier or a perforated foil radiant barrier was implemented at the substrate of a R-19 fiberglass insulation batt. The addition of a plastic vapor barrier at the substrate reduced the total heat transfer by 13% when compared to a no vapor barrier case. It is significant to realize that a 13% (measured data) decrease in the total heat transferred through the ceiling into a home during the summer season can help the overall national energy savings and pollution reduction. The authors have found in previous works Refs. [2-3], that moisture is insignificant in the winter, which would imply that the vapor barrier would have a negligible effect. With the addition of either a perforated or a non-perforated radiant barrier at the substrate the total heat transfer essentially did not change when

compared to the no vapor barrier and plastic vapor barrier cases, respectively. As demonstrated, the use of a radiant barrier substrate will have essentially no effect (less than 1%). However as discussed in the results the different modes of heat transfer were strongly affected when each of these substrate radiant barriers were added. Use of substrate vapor barriers, being plastic or non-perforated foil, was found to reduce the total heat transfer into the living area of a residential home as compared to the case of a standard R-19 fiberglass batt without any vapor barrier. Further, this paper investigated the results of combining a vapor barrier to the substrate and a radiant foil barrier above the fiberglass insulation. This combination resulted in a total heat transfer reduction of 53% (experimental data) when compared to a standard R-19 insulation batt. A 53% reduction in the total heat transfer through the ceiling into the home can make a considerable savings in energy consumption.

REFERENCES

[1] Levins, W.P., Karnitz, M.A., and Hall, J.A., "Moisture Measurements in Single-Family Houses with Attics Containing Radiant Barriers", Oak Ridge National Laboratory, Report ORNL/CON-255, February 1989.

[2] Gorthala, R., Roux, J. A. and Fairey III, P. W.,"Combined Conduction, Radiation Heat Transfer and Mass Transfer in Fibrous Attic Insulations," Insulation Materials: Testing and Applications, 2nd Volume, ASTM STP 111, American Society for Testing and Materials, Philadelphia, 1991, pp. 371-386.

[3] Harris, K.T., McCarty, T.A., Roux, J.A., and Gorthala, R., "Total Heat Transfer Due to the Variation in Fiberglass Insulation Thickness in Attics," ASME National Conference on Heat Transfer, August 8-11, 1993, Radiative Heat Transfer Theory and

Applications, HTD-Vol. 244, pp. 1-10.

[4] Gorthala, R., Harris, K.T., Roux, J.A., and McCarty, T.A., "Transient, Conductive, Radiative Heat Transfer Coupled with Moisture Transport in Attic Insulations," Journal of Thermophysics and Heat Transfer, Vol. 8, No. 1, Jan.-Mar. 1994.

[5] Yarbough, D., Personal contact, Oak Ridge National Laboratory, March 1994.

[6] Wilks, K., Personal Contact, Oak Ridge National Laboratory, June 1994.

[7] Fairey, P., Personal Contact, Florida Solar Energy Center, June 1994.

[8] Hust, J. G., Callanan, J. E., and Sullivan, S. A.,"Specific Heat of Insulations," Thermal Conductivity 19, D. W., Yarbrough, Ed., Plenum, N.Y., 1988, pp. 533-550.

[9] Yeh, H. Y., and Roux, J. A., "Spectral Radiative Properties of Fiberglass Insulation", Journal of Thermophysics and Heat Transfer, Vol. 2, No. 1, January 1988, pp. 75-81.

[10] Roux, J. A., Smith, A. M., and Todd, D. C., "Radiative Transfer with Anisotropic Scattering and Arbitrary Temperature for Plane Geometry," AIAA Journal, Vol. 13, No. 9, Sept. 1975, pp.1203-1211.

[11] Rish, J.W. and Roux, J.A., 1987 "Heat Transfer Analysis of Fibrous Insulations With and Without Radiant Barriers for Summer Conditions," Journal of Thermophysics and Heat Transfer, 1(1):43-49

[12] Hansen, K. K.,"Sorption Isotherms," A Catalogue, 1985, Building Materials Laboratory, Department of Civil Engineering, The Technical University of Denmark.

[13] Tchernev, D.I., "Exploration of Molecular Sieve Zelolites for the Cooling of Buildings with Solar Energy," Report: NSF/RA - 770017.

[14] Tchernev, D.I.,"Solar Energy Application of Natural Zeolites," Natural Zeolite and Its

Use, Oxford, New York, Pergamon Press, 1978, pp. 479-484.

[15] Langlais, C., Hyrien, C., Klarsfeld, S., 1982,"Moisture Migration in Fibrous Insulating Materials under the Influence of a Thermal Gradient and Its Effect on Thermal Resistance," Moisture Migration in Buildings,ASTM STP 779, pp. 191-206.

[16] Patankar, S. V., Numerical Heat Transfer and Fluid Flow, Hemisphere Publishing Corp., Washington, D.C., 1980.

[17] Houston, R.L. and S.A. Korpela, 1982, "Heat Transfer Through Fiberglass Insulation", Proceeding of the 7th International Heat Transfer Conference, 2:449-504

[18] Yajinik, S. J.A. Roux 1986, " Determination of Radiative Properties of Fiberglass and Foam Insulation," Report ORNL/Sub/86-55930/1, Oak Ridge National Laboratory.

[19] Holman, J.P., 1990, Heat Transfer, 7th Ed. McGraw-Hill Publishing.

[20] Tao, Y.X., R.W. Besant and K.S. Rezkallah, 1992, "Transient Thermal Response of a Glass-Fiber Insulation Slab with Hygroscope Effects", International Journal of Heat and Mass Transfer, 35(5):1155-1167

TABLE 1. Radiative and thermal properties used in numerical computations.

ρ_f[a]	12.0	kg/m^3
c_f[a]	844.4	J/kg-K
k_f[b]	$a + bT + 8.5537 \times 10^{-5} \rho_f$ $a = 4.97576 \times 10^{-3}$, $b = 7.00025 \times 10^{-5}$	W/m-K
ω[c]	0.201	
β[c]	3.70	cm^{-1}
γ_{vr}[d]	1.2×10^{-5}	m^2/s
γ_b[e]	1.19×10^{-9}	m^2/s
m_ϕ[f]	$1/100 \quad .10 \leq \phi \leq .90$	
γ_v/γ_{vr}[d]	$(T/T_r)^{1.5}$	

[a]Ref.[8], [b]Ref.[17], [c]Ref.[18], [d]Ref.[19], [e]Ref.[20], [f]Ref.[12]

subscript r represents referenced values.

TABLE 2. Time integrated substrate heat flux corresponding to R-19 fiberglass batt with a plastic vapor barrier or non-perforated foil radiant barrier or a perforated foil radiant barrier for summer conditions.

Date	Plastic Vapor Barrier	Substrate Radiant Barrier	Case	Heating[a] Portion R-19 kJ/m^2
7/27/94	With		Model	-38.3
			Data	-41.8 [13%][b]
		Non-Perforated	Model	-38.2
			Data	-----
7/27/94	Without		Model	-49.6
			Data	-48.1
		Perforated	Model	-49.6
			Data	-----
6/25/94	With/Vapor Barrier Below With/Radiant Barrier Above		Model	-19.1
			Data	-24.7 [53%][b]
	Standard R-19 Batt		Model	-47.7
			Data	-53.2

[a]Integrated over heat gain period (550 min $<$ t $<$ 1210 min).

[b]Reduction in substrate heat flux when comparing vapor and no vapor barrier cases.

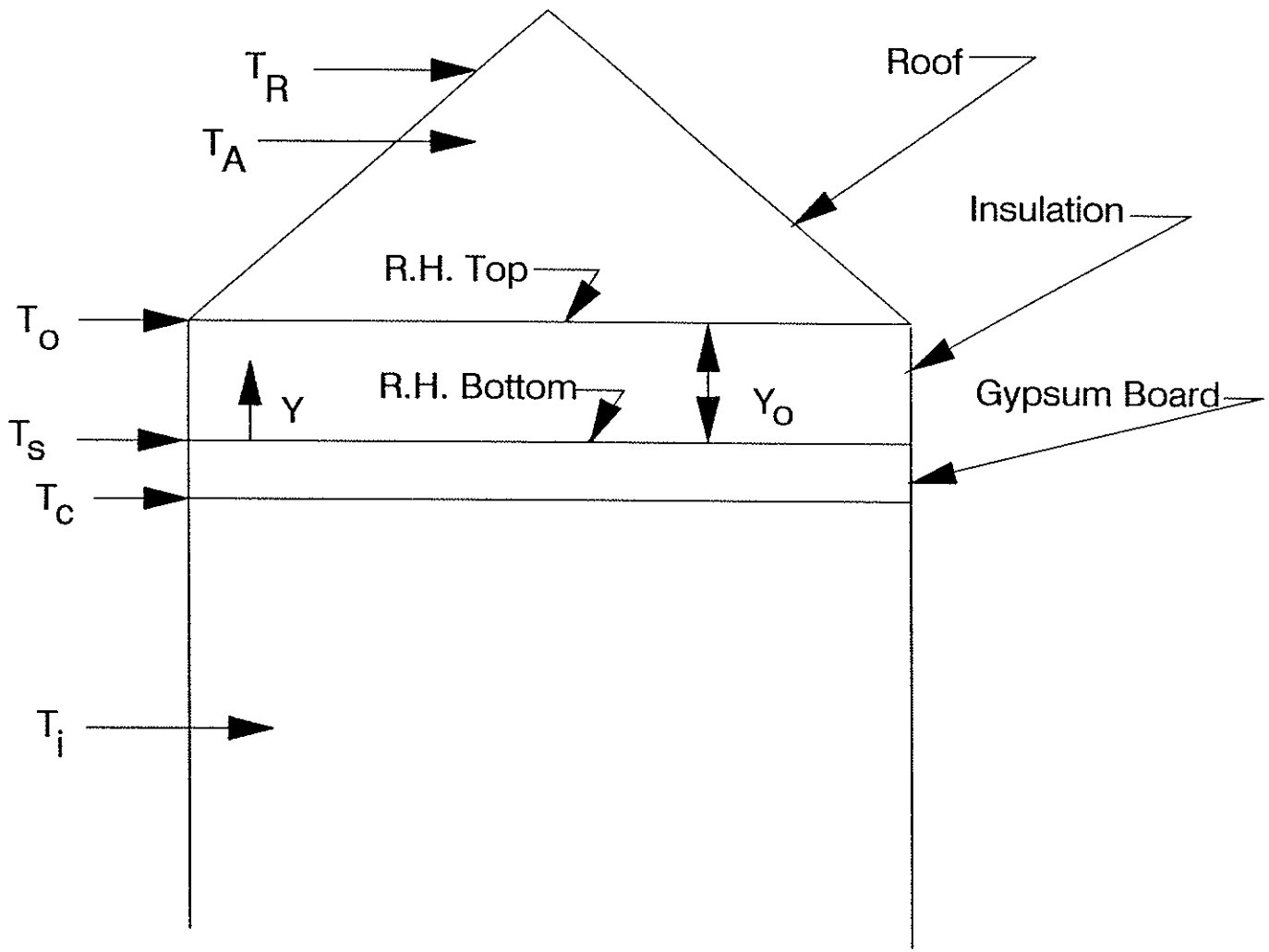

Fig. 1 Attic sketch.

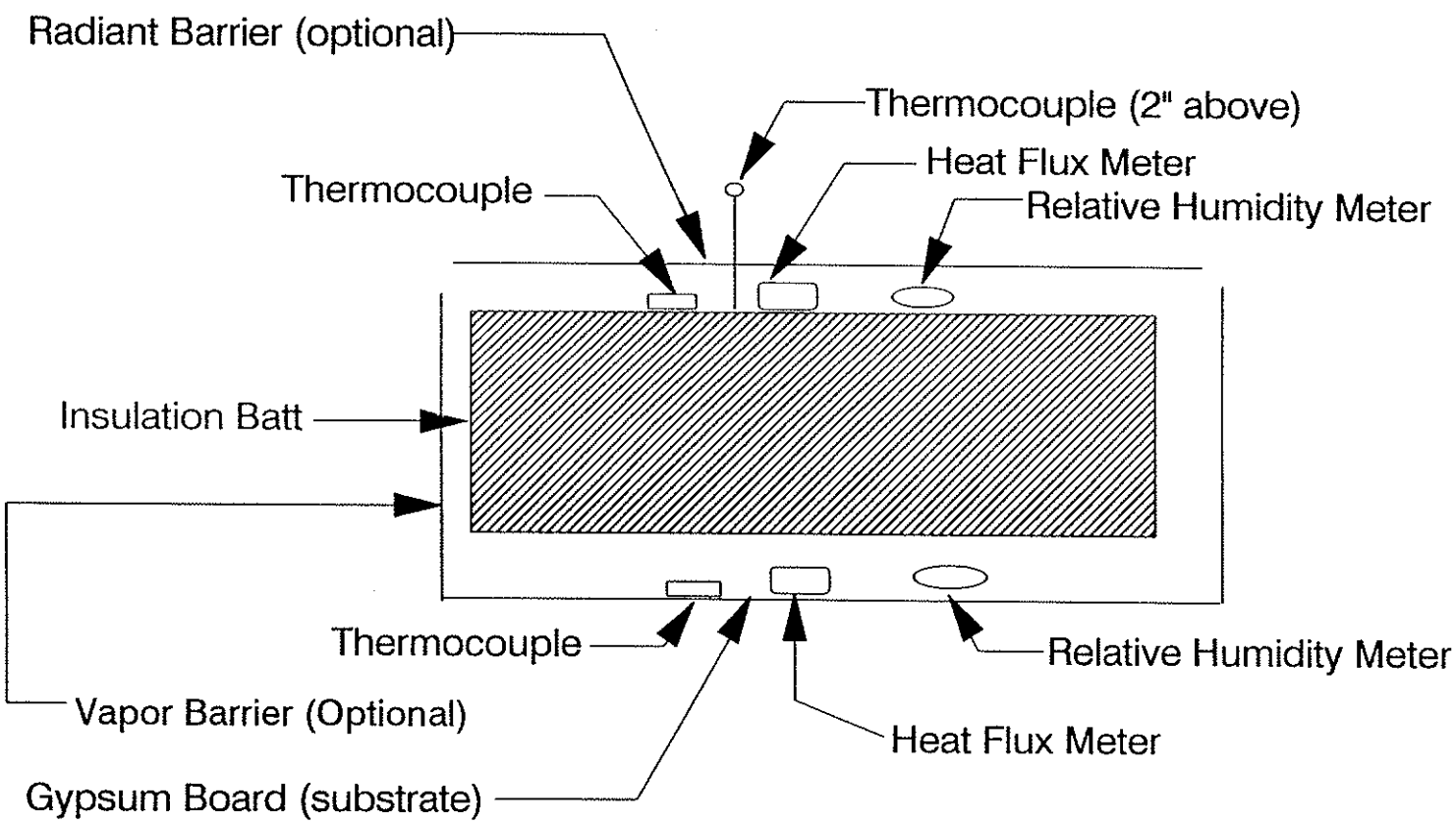

Fig. 2 Location of heat flux meters, relative humidity meters and thermocouples about the insulation batt.

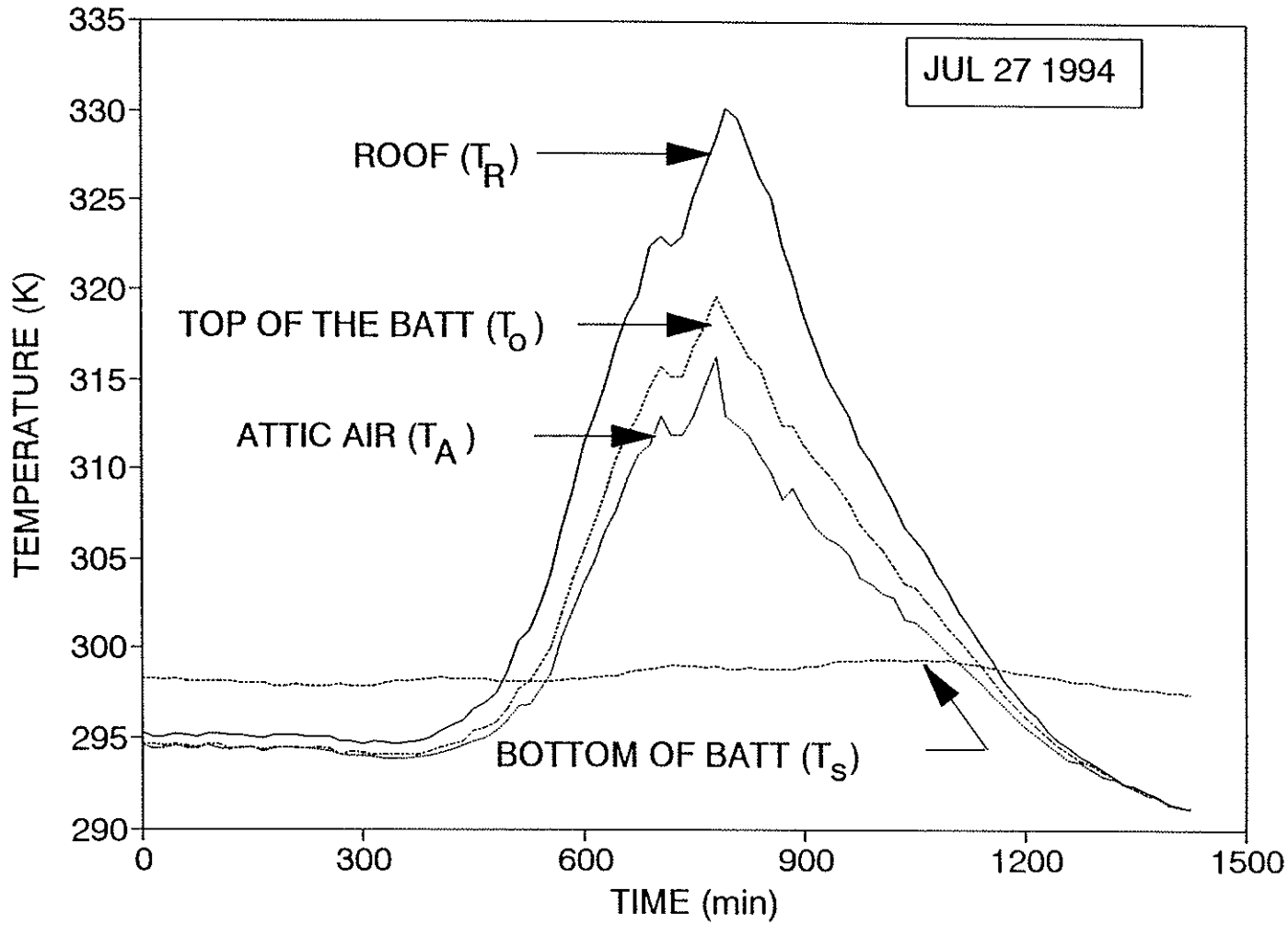

FIGURE 3. Temperature-time histories for a R-19 fiberglass insulation batt with a plastic vapor barrier at the substrate.

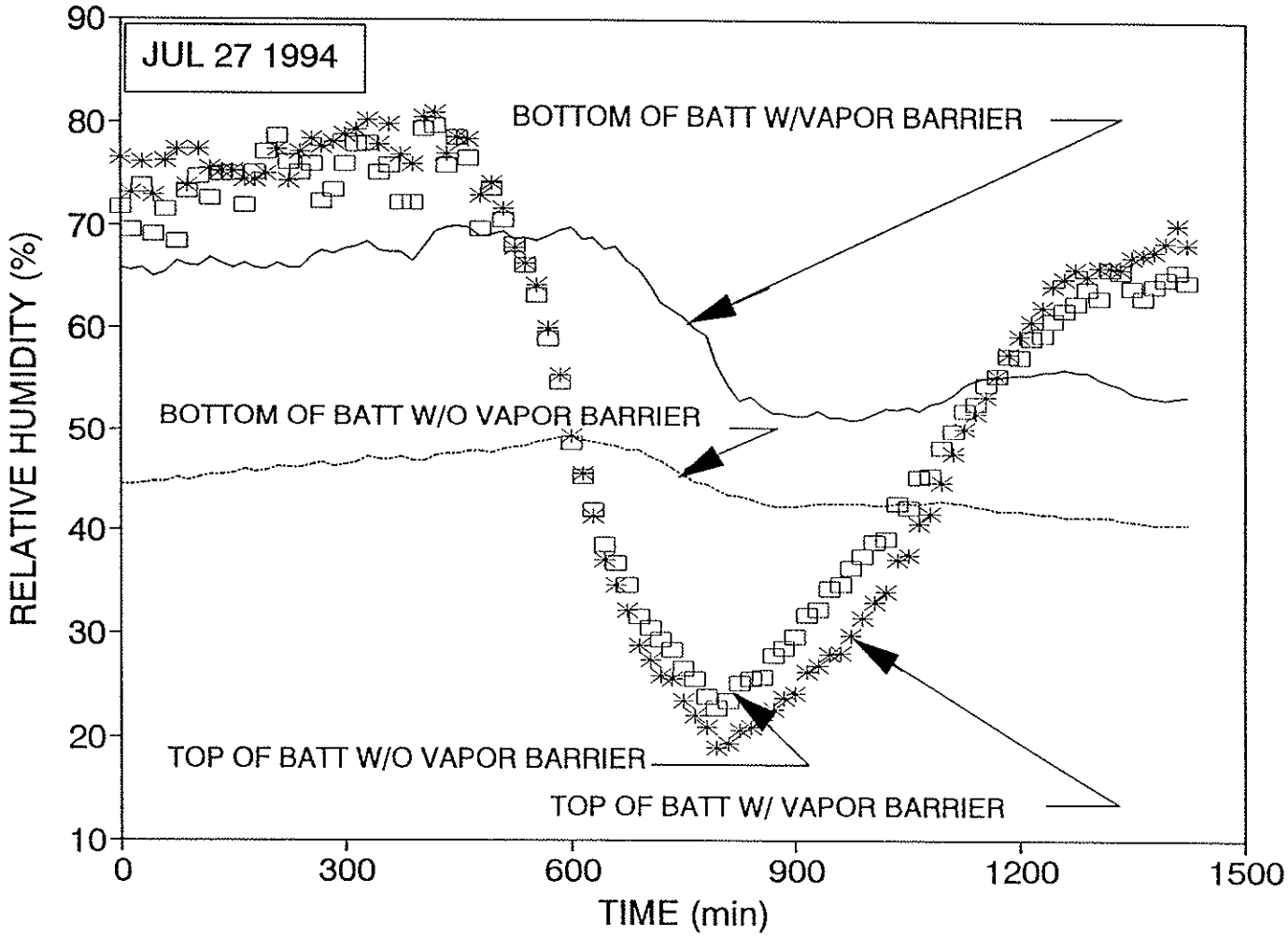

FIGURE 4. Measured relative humidities at different locations of the insulation for both batts with and without a plastic vapor barrier.

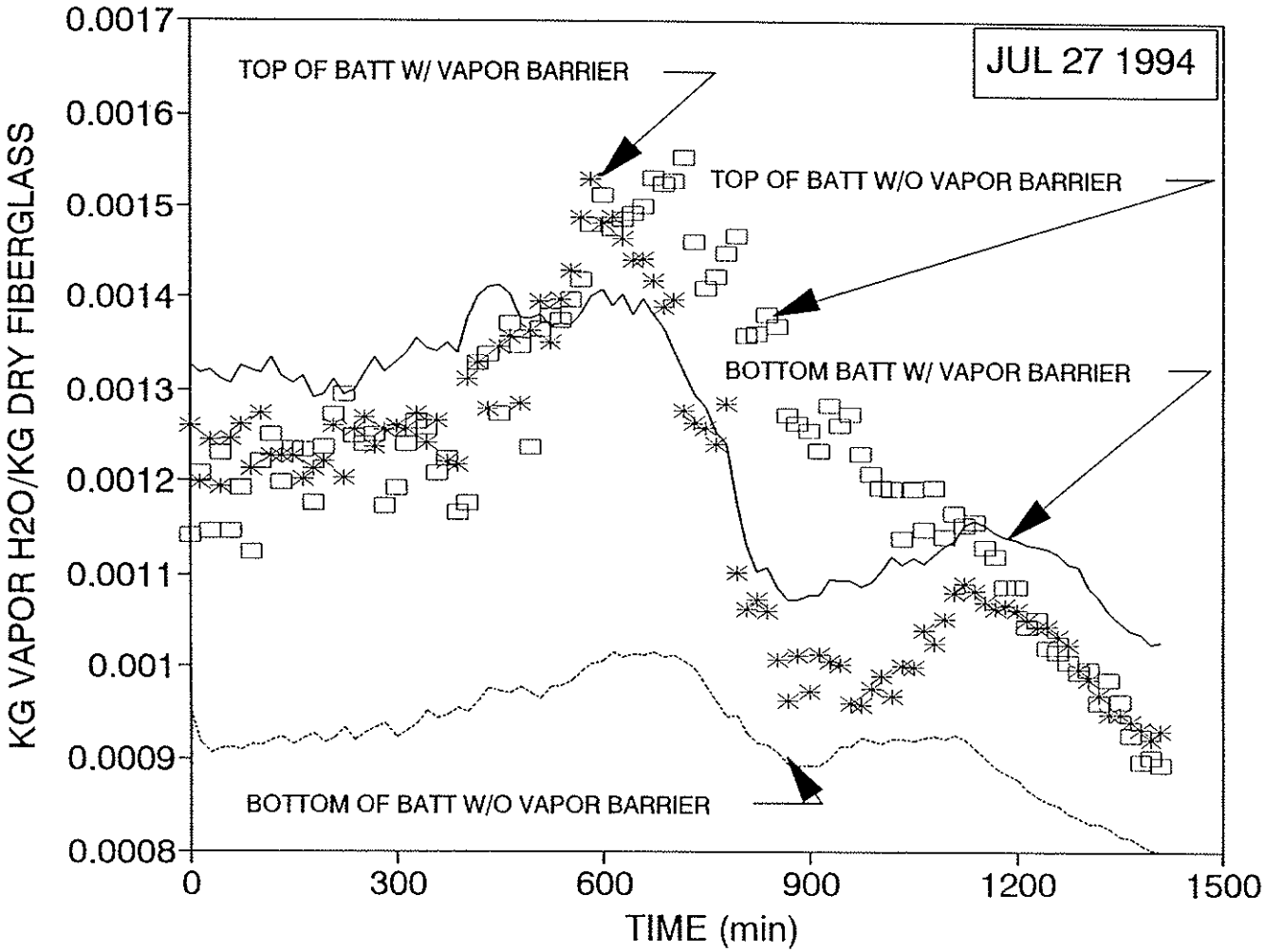

FIGURE 5. Vapor H2O concentration histories for both batts with and without a plastic vapor barrier at the insulation substrate.

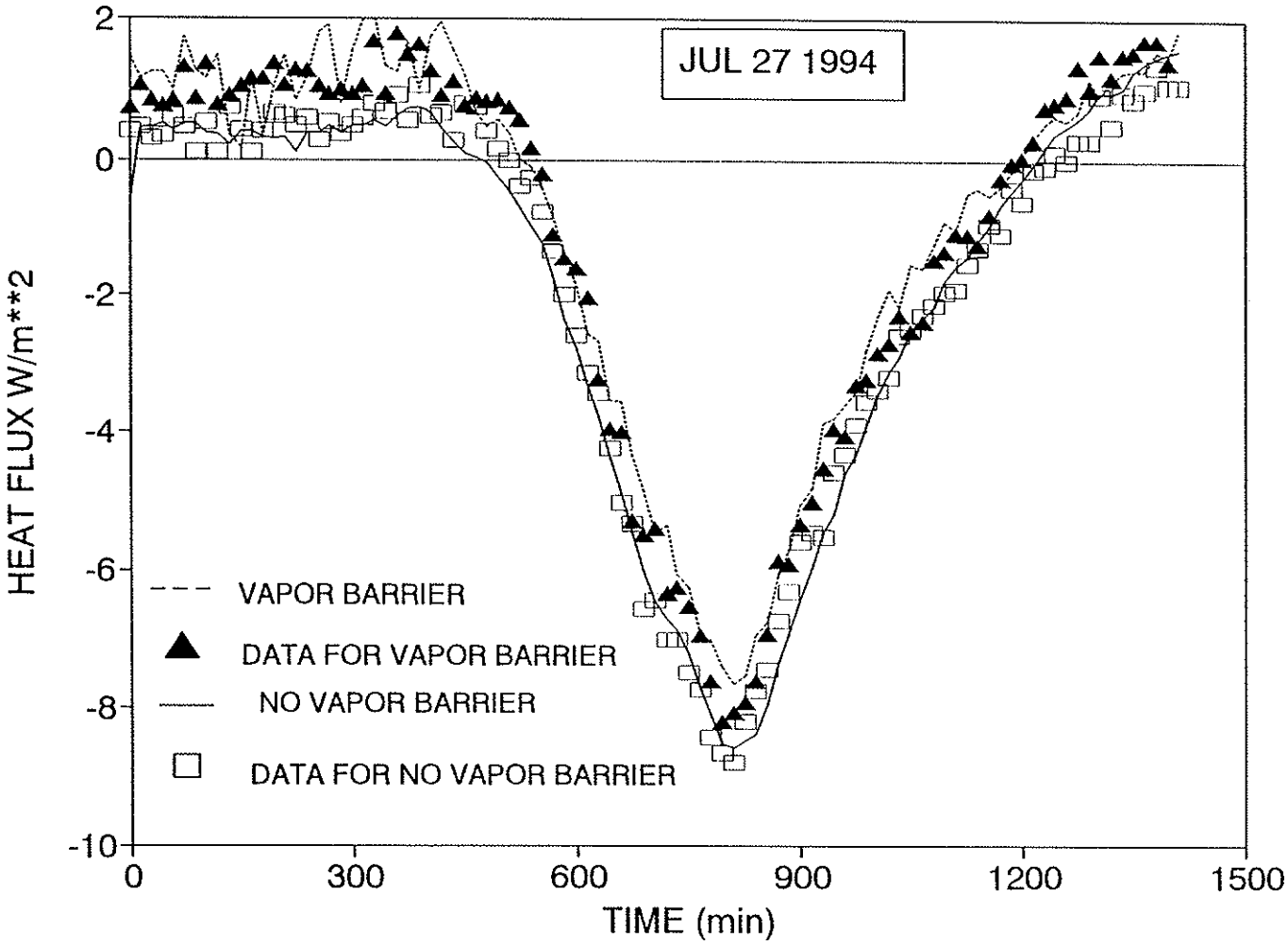

FIGURE 6. Substrate measured and predicted heat flux-time histories for both cases with and without a plastic vapor barrier.

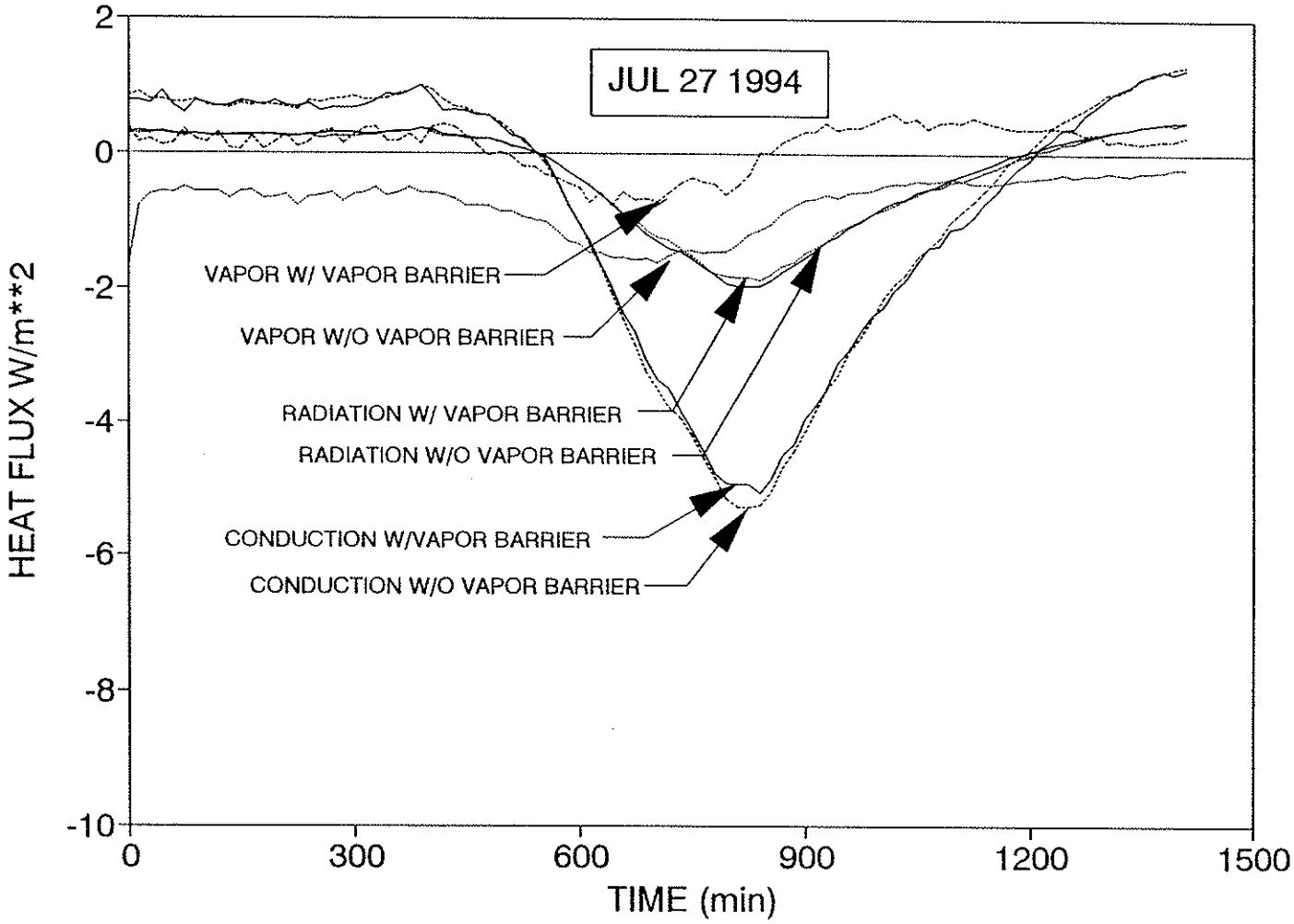

FGURE 7. Predicted substrate heat flux-time histories for the conduction, radiation, and vapor H2O diffusion modes.

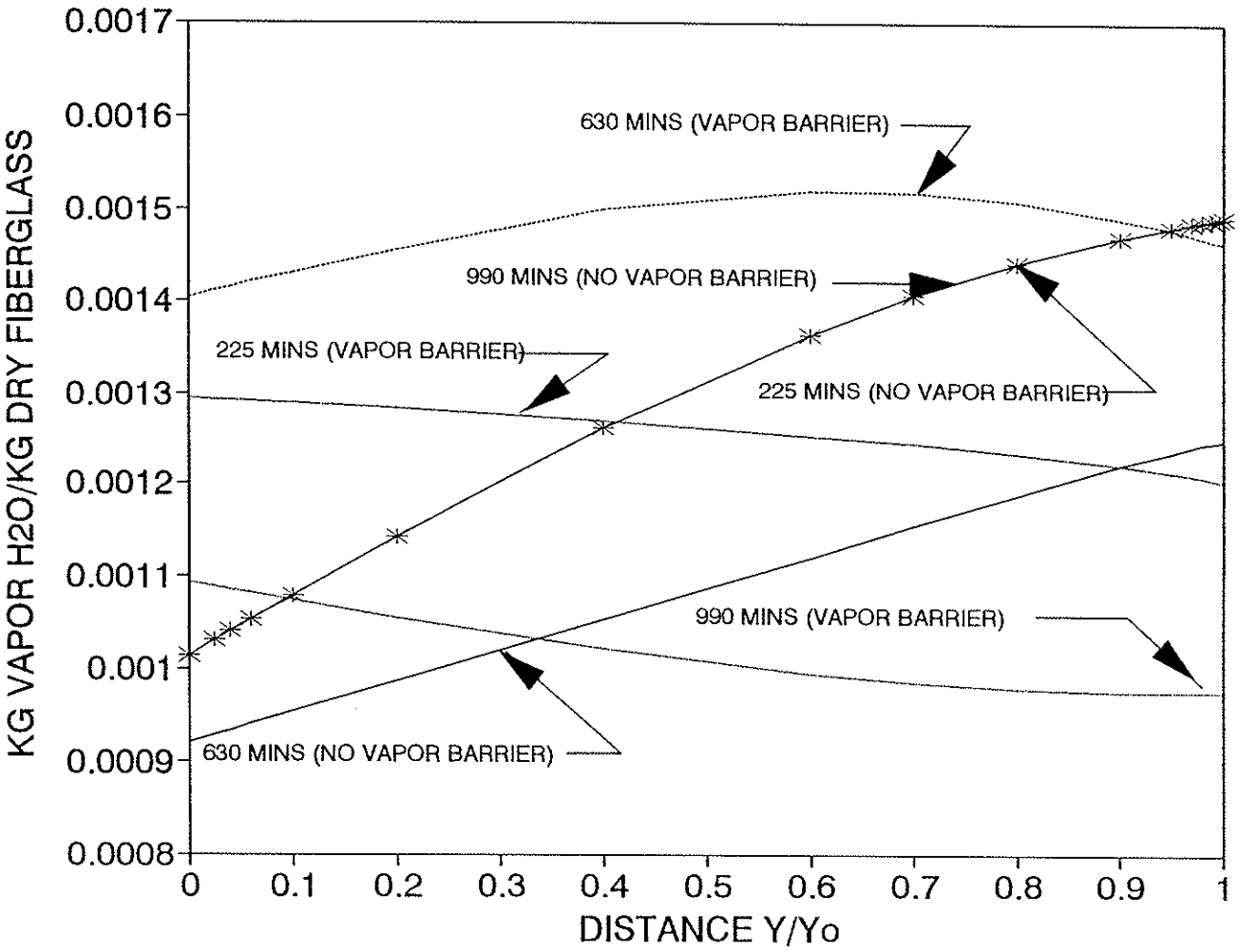

FIGURE 8. Spatial concentration profiles for different time instances for R-19 insulation with and without a plastic vapor barrier.

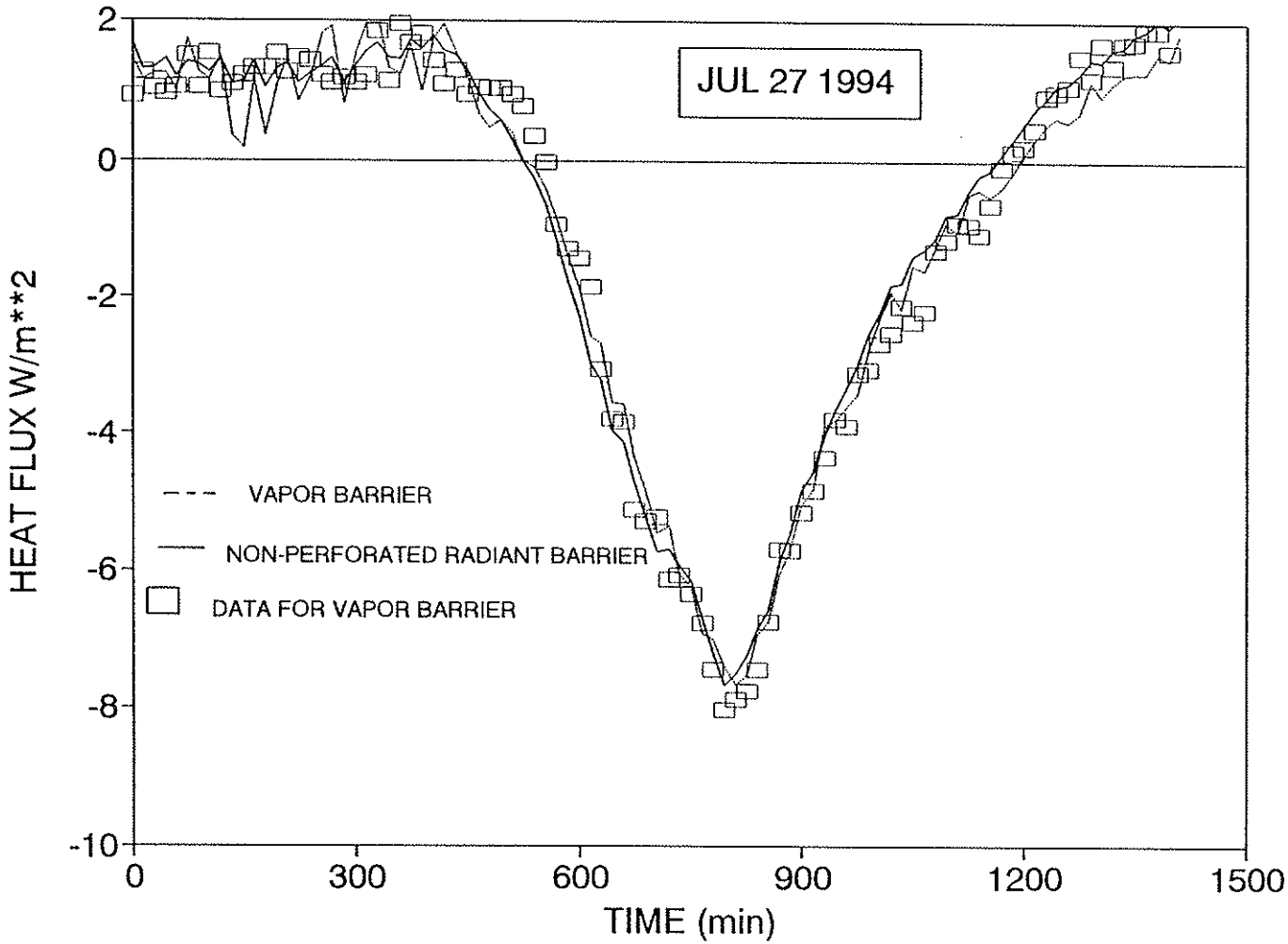

FIGURE 9. Substrate measured and predicted heat flux -time histories for both with and without a non-perforated radiant barrier.

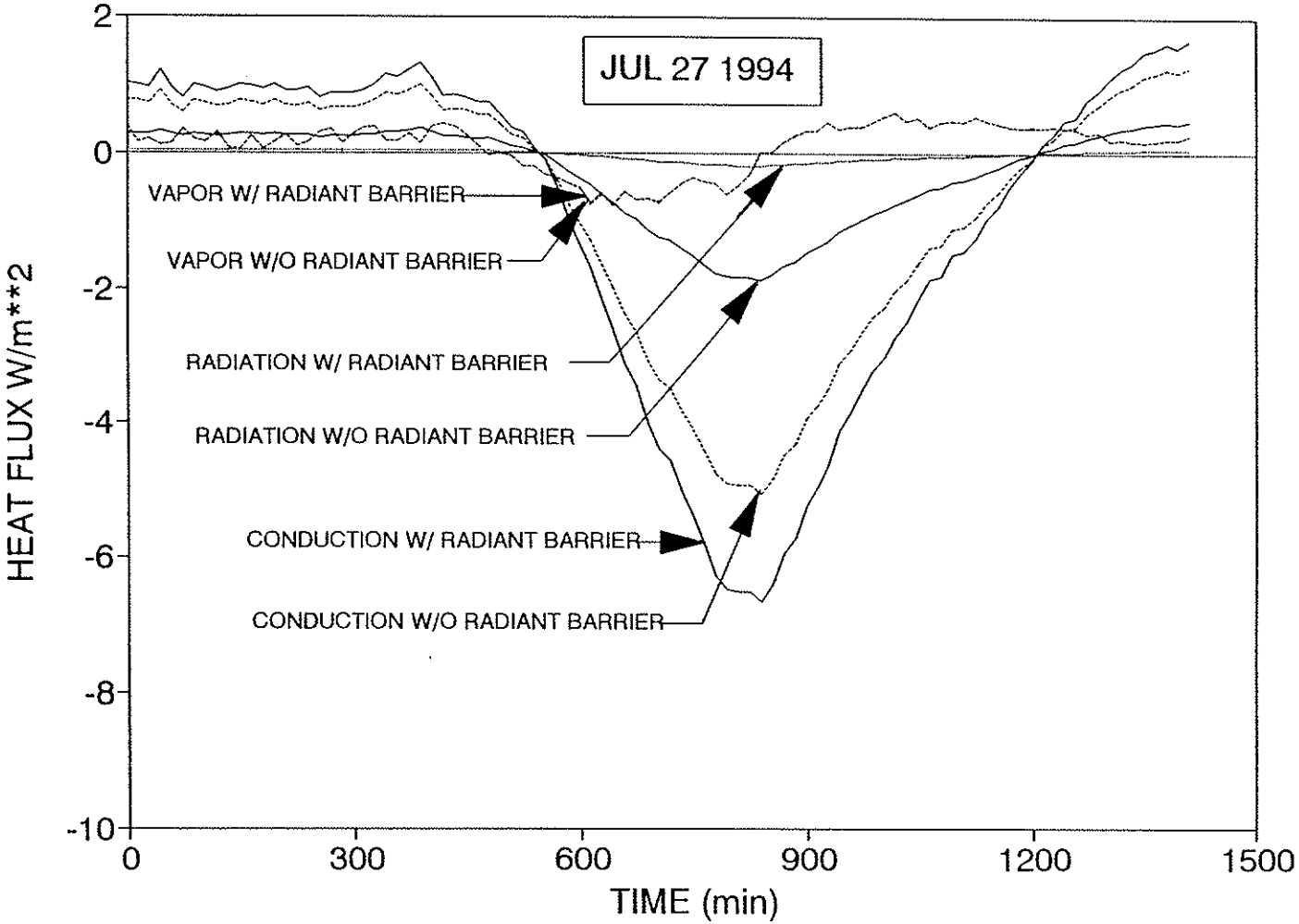

FIGURE 10. Predicted substrate heat flux-time histories for the conduction, radiation, and vapor H2O diffusion modes for a batt with and without a non-perforated radiant barrier.

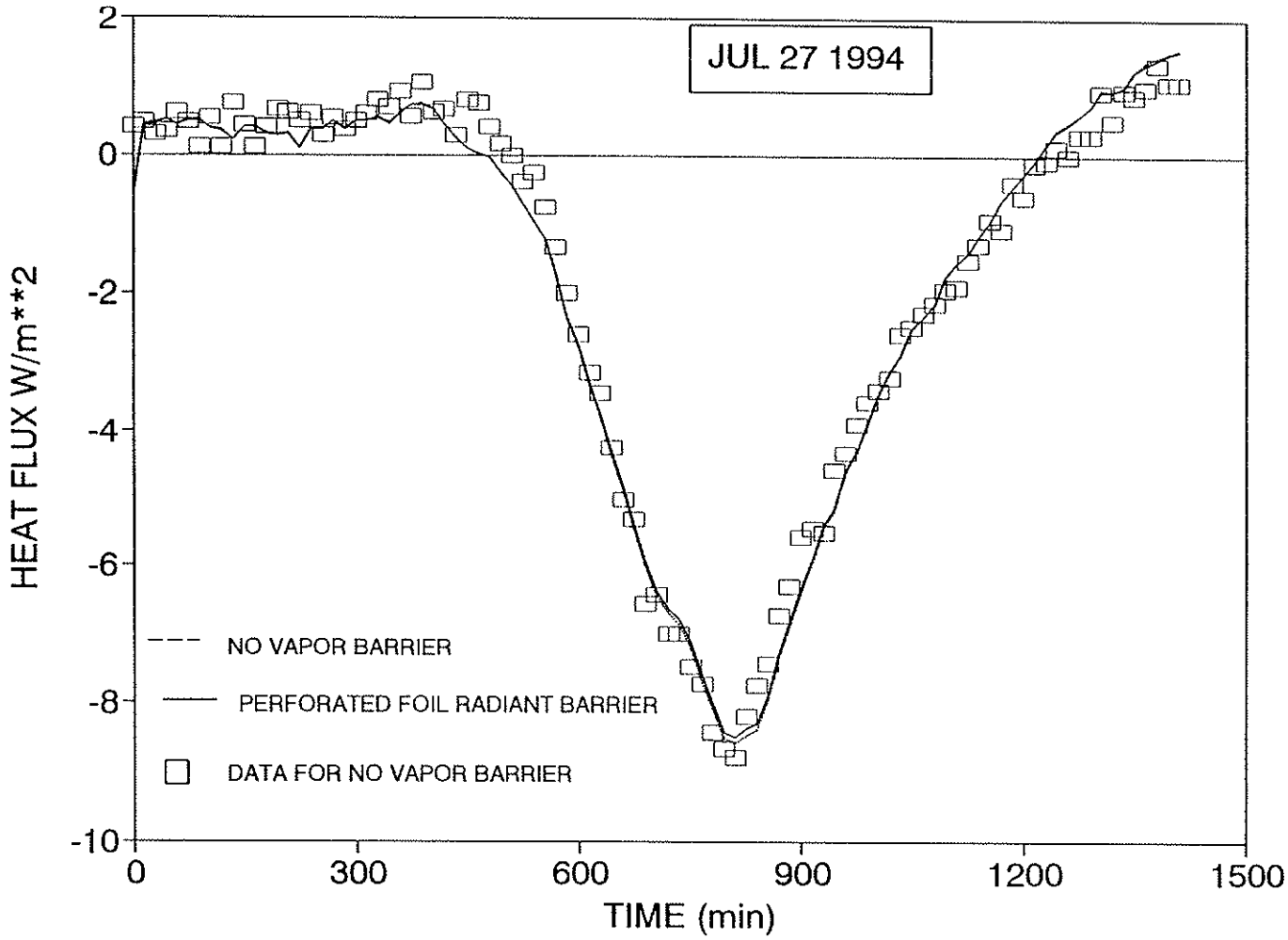

FIGURE 11. Substrate measured and predicted heat flux-time histories for both with and without perforated radiant barrier.

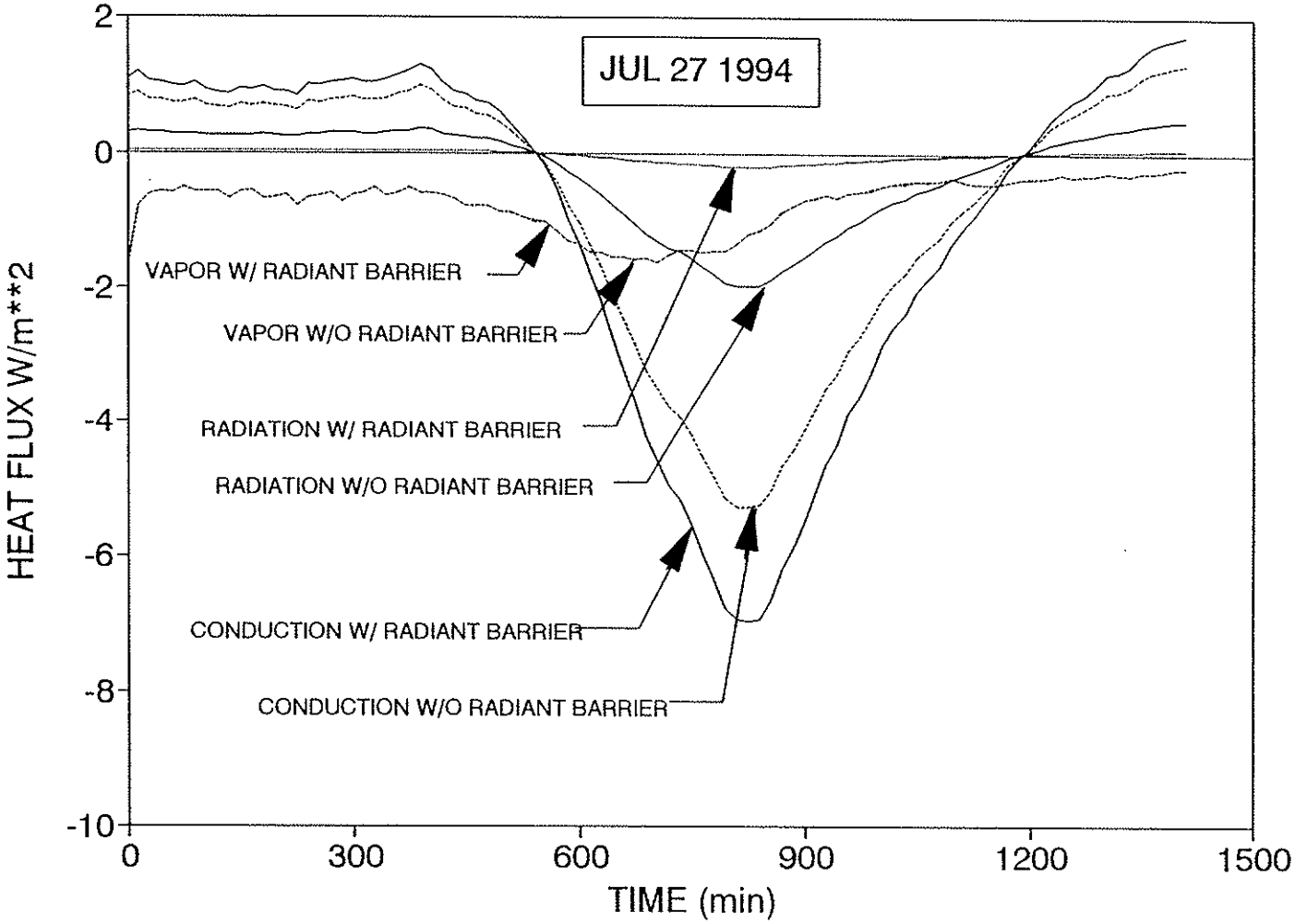

FIGURE 12. Predicted substrate heat flux-time histories for the conduction, radiation, and H2O vapor diffusion modes for a batt with and without a perforated radiant barrier.

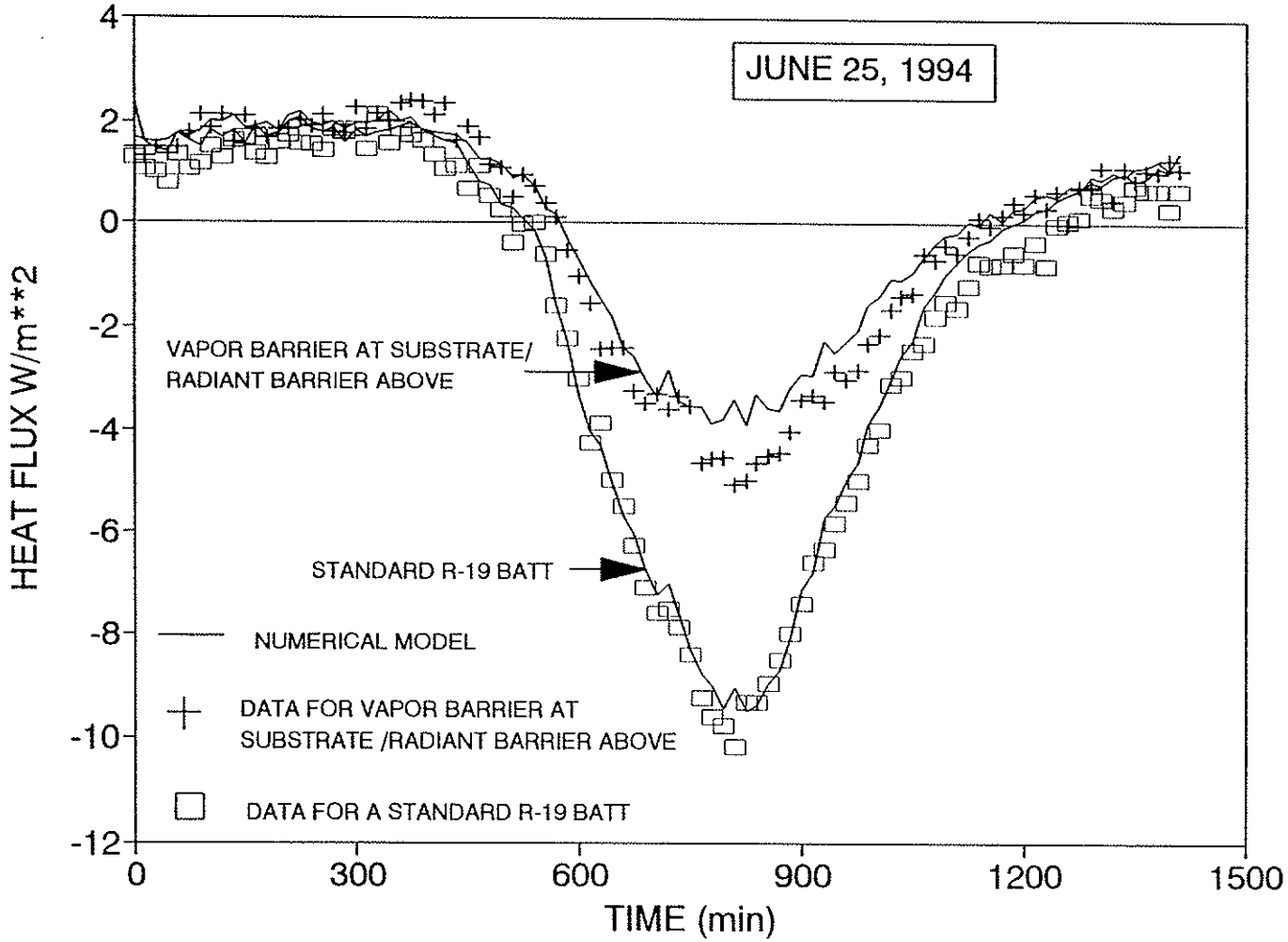

FIGURE 13. Substrate measured and predicted heat flux histories for a batt with a plastic vapor barrier at the substrate and a radiant foil barrier above as compared to a standard R-19 insulation batt.